First publ. in: Optics Express 15 (2007), 11, pp. 6643-6650

Activity of the human visual cortex measured non-invasively by diffusing-wave spectroscopy

Franck Jaillon, Jun Li, Gregor Dietsche, Thomas Elbert[†] and Thomas Gisler

Universität Konstanz, Fachbereich Physik, 78457 Konstanz, Germany
[†]Universität Konstanz, Fachbereich Psychologie, 78457 Konstanz, Germany
thomas.gisler@uni-konstanz.de

Abstract: Activity of the human visual cortex, elicited by steady-state flickering at 8 Hz, is non-invasively probed by multi-speckle diffusing-wave spectroscopy (DWS). Parallel detection of the intensity fluctuations of statistically equivalent, but independent speckles allows to resolve stimulation-induced changes in the field autocorrelation of multiply scattered light of less than 2%. In a group of 9 healthy subjects we find a faster decay of the field autocorrelation function during the stimulation periods for data measured with a long-distance probe (30 mm source-receiver distance) at 2 positions over the occipital cortex (t-test: $t(8) = -2.672$, $p = 0.028 < 0.05$ for position 1, $t(8) = -2.874$, $p = 0.021 < 0.05$ for position 2). In contrast, no statistically significant change is seen when a short-distance probe (16 mm source-receiver distance) is used (t-test: $t(8) = -2.043$, $p = 0.075 > 0.05$ for position 1, $t(8) = -2.146$, $p = 0.064 > 0.05$ for position 2). The enhanced dynamics observed with DWS is positively correlated with the functional increase of blood volume in the visual cortex, while the heartbeat rate is not affected by stimulation. Our results indicate that the DWS signal from the visual cortex is governed by the regional cerebral blood flow velocity.

OCIS codes: (030.6140) Speckle; (170.0170) Medical optics and biotechnology; (170.5270) Photon density waves; (170.5280) Photon migration; (290.1990) Diffusion; (290.1350) Backscattering; (290.4210) Multiple Scattering; (290.7050) Turbid media

References and links

1. K. Dörschel and G. Müller, "Velocity resolved laser Doppler blood flow measurements in skin," Flow Meas. Instrum. **7**, 257–264 (1996).
2. G. Maret and P. E. Wolf, "Multiple light scattering from disordered media: The effect of Brownian motion of scatterers," Z. Phys. B **65**, 409–413 (1987).
3. D. J. Pine, D. A. Weitz, P. M. Chaikin, and E. Herbolzheimer, "Diffusing-Wave Spectroscopy," Phys. Rev. Lett. **60**, 1134–1137 (1988).
4. C. Menon, G. M. Polin, I. Prabakaran, A. Hsi, C. Cheung, J. P. Culver, J. F. Pingpank, C. S. Sehgal, A. G. Yodh, D. G. Buerk, and D. L. Fraker, "An integrated approach to measuring tumor oxygen status using Human Melanoma Xenografts as a Model," Cancer Res. **63**, 7232–7240 (2003).
5. G. Yu, T. Durduran, C. Zhou, H.-W. Wang, M. E. Putt, H. M. Saunders, C. S. Sehgal, E. Glatstein, A. G. Yodh, and T. M. Busch, "Noninvasive monitoring of murine tumor blood flow during and after photodynamic therapy provides early assessment of therapeutic efficacy," Clin. Cancer Res. **11**, 3543–3552 (2005).

Konstanzer Online-Publikations-System (KOPS)
URL: http://www.ub.uni-konstanz.de/kops/volltexte/2008/5440/
URN: http://nbn-resolving.de/urn:nbn:de:bsz:352-opus-54408

6. U. Sunar, H. Quon, T. Durduran, J. Zhang, J. Du, C. Zhou, G. Q. Yu, R. Choe, A. Kilger, R. Lustig, L. Loevner, S. Nioka, B. Chance, and A. G. Yodh, "Noninvasive diffuse optical measurement of blood flow and blood oxygenation for monitoring radiation therapy in patients with head and neck tumors: a pilot study," J. Biomed. Opt. **11**, 064,021 (2006).
7. G. Yu, T. Durduran, C. Zhou, T. C. Zhu, J. C. Finlay, T. M. Busch, S. B. Malkowicz, S. M. Hahn, and A. G. Yodh, "Real-time in Situ monitoring of Human Prostate Photodynamic Therapy with Diffuse Light," Photochem. Photobiol. **82**, 1279–1284 (2006).
8. T. Durduran, R. Choe, G. Yu, C. Zhou, J. C. Tchou, B. J. Czerniecki, and A. G. Yodh, "Diffuse optical measurements of blood flow in breast tumors," Opt. Lett. **30**, 2915–2917 (2005).
9. G. Yu, T. Durduran, G. Lech, C. Zhou, B. Chance, E. R. Mohler III, and A. G. Yodh, "Time-dependent blood flow and oxygenation in human skeletal muscles measured with noninvasive near-infrared diffuse optical spectroscopies," J. Biomed. Opt. **10**, 024,027–1–12 (2005).
10. G. Yu, T. F. Floyd, T. Durduran, C. Zhou, J. Wang, J. A. Detre, and A. G. Yodh, "Validation of diffuse correlation spectroscopy for muscle blood flow with concurrent arterial spin labeled perfusion MRI," Opt. Express **15**, 1064–1075 (2007).
11. T. Durduran, G. Yu, M. G. Burnett, J. A. Detre, J. H. Greenberg, J. Wang, C. Zhou, and A. G. Yodh, "Diffuse optical measurement of blood flow, blood oxygenation, and metabolism in a human brain during sensorimotor cortex activation," Opt. Lett. **29**, 1766–1768 (2004).
12. J. Li, G. Dietsche, D. Iftime, S. E. Skipetrov, G. Maret, T. Elbert, B. Rockstroh, and T. Gisler, "Non-Invasive detection of functional brain activity with near-infrared diffusing-wave spectroscopy," J. Biomed. Opt. **10**, 044,002–1–12 (2005).
13. P. E. Roland, B. Larsen, N. A. Lassen, and E. Skinhøj, "Supplementary motor area and other cortical areas in Organization of Voluntary Movements in Man," J. Neurophysiol. **43**, 118–136 (1980).
14. R. J. Seitz and P. E. Roland, "Learning of sequential finger movements in man: A Combined Kinematic and Positron Emission Tomography (PET) Study," Eur. J. Neurosci. **4**, 154–165 (1992).
15. M. A. Franceschini, S. Fantini, J. J. Thompson, J. P. Culver, and D. A. Boas, "Hemodynamic evoked response of the sensorimotor cortex measured non-invasively with near-infrared optical imaging," Psychophysiol. **40**, 548–560 (2003).
16. During finger opposition for 130 s which leads to a reduction of the DWS decay time measured over the somatomotor area C3 by about 28%, we observe heartbeat increases of typically 20% (J. Li et al., unpublished data).
17. M. A. Pastor, J. Artieda, J. Arbizu, M. Valencia, and J. C. Masdeu, "Human cerebral activation during steady-state visual-evoked responses," J. Neurosci. **23**, 11,621–11,627 (2003).
18. C. S. Herrmann, "Human EEG responses to 1-100 Hz flicker: resonance phenomena in visual cortex and their potential correlation to cognitive phenomena," Exp. Brain Res. **137**, 346–353 (2001).
19. H. Ito, K. Takahashi, J. Hatazawa, S.-G. Kim, and I. Kanno, "Changes in Human regional cerebral blood flow and cerebral blood volume during Visual stimulation measured by Positron Emission Tomography," J. Cereb. Blood Flow Metab. **21**, 608–612 (2001).
20. F. B. Mohamed, A. B. Pinus, S. H. Faro, D. Patel, and J. I. Tracy, "BOLD fMRI of the visual cortex: Quantitative responses measured with a graded stimulus at 1.5 Tesla," J. Magn. Reson. **16**, 128–136 (2002).
21. H. H. Jasper, "The ten-twenty electrode system of the International Federation," Electroencephal. Clin. Neurophysiol. **10**, 370–375 (1958).
22. T. Gisler, H. Rüger, S. U. Egelhaaf, J. Tschumi, P. Schurtenberger, and J. Rička, "Mode-selective dynamic light scattering: theory versus experimental realization," Appl. Opt. **34**, 3546–3553 (1995).
23. D. E. Koppel, "Statistical accuracy in fluorescence correlation spectroscopy," Phys. Rev. A **10**, 1938–1945 (1974).
24. E. Okada and D. T. Delpy, "Near-infrared light propagation in an adult head model. II. Effect of superficial tissue thickness on the sensitivity of the near-infrared spectroscopy signal," Appl. Opt. **42**, 2915–2922 (2003).

1. Introduction

When tissue is illuminated by light with large coherence length, a speckle pattern forms on the surface which arises from the interference of multiply scattered photons which have travelled through the tissue along different paths. Fluctuations of the speckle intensity $I(\boldsymbol{r},t)$ at the position $\boldsymbol{r}$ yield information on microscopic motions of scatterers within the volume swept by the diffuse photon cloud. In contrast to laser Doppler velocimetry where the power spectrum of speckle fluctuations measured in near-backscattering geometry is dominated by skin blood flow [1], diffusing-wave spectroscopy (DWS [2, 3]; also called diffuse correlation spectroscopy, DCS) measures the temporal intensity autocorrelation function $g^{(2)}(\tau) = \langle I(0)I(\tau)\rangle / \langle |I(0)|\rangle^2$ at large source-receiver distances of up to several centimeters. The high sensitivity to even minute scatterer displacements has lead to several applications of DWS in the fields of tumor

and skeletal muscle perfusion [4, 5, 6, 7, 8, 9, 10].

Recently, DWS was used to non-invasively detect functional activity in the human somato-motor cortex [11, 12]. The analysis of DWS autocorrelation functions yielded a increase of the cortical dynamics of about 40% upon contralateral stimulation by a finger opposition exercise. The enhanced dynamics in the somato-motor cortex observed with DWS is consistent with the activation-induced increase of cerebral blood flow (CBF) observed with positron emission tomography (PET) [13, 14]. While the coupling of blood flow velocity and the DWS signal has been validated in skeletal muscle [10], the origin of the DWS signal from the cortex is not understood in detail. As cortical tissue is strongly scattering, DWS could, in addition to blood flow velocity, also be sensitive to shear deformations within the tissue surrounding the vessels which are induced by pulsation. Motor stimulation is not suited to assess the contributions of blood flow velocity and tissue shearing to the DWS signal separately since both the blood flow velocity and the heartbeat rate (which governs the shear rate within tissue) change simultaneously [12, 15, 16].

Steady-state flickering elicits a strong oscillatory response in the primary visual cortex and has been extensively studied with electroencephalography (EEG) [17, 18]. PET experiments show that 8 Hz flickering may induce an increase of the cerebral blood flow of 68%, and an increase of the cerebral blood volume (CBV) of as much as 21% [19]. In contrast to motor stimulation, heartbeat rate changes during flickering stimulation are very small [19], which makes this protocol a good candidate for studying the effect of functionally enhanced blood flow on the DWS signal without interfering effects from tissue shearing. The primary visual cortex is located around the calcarine fissure in the occipital lobe, with a substantial portion inside the sulcus and the medial aspects of both hemispheres, i.e., at a considerable distance from the surface. Functional MRI data indicate that the spatial dimension of activated areas in the primary visual cortex increases with the intensity contrast of the stimulus [20]. Given the low signal-to-noise ratio of DWS autocorrelation functions resulting from the large source-receiver distance required for probing the cortex, the detection of activity in the primary visual cortex areas with DWS presents a serious challenge to currently used fiber-based detection schemes.

In this paper, we report on the non-invasive detection of functional activity in the primary visual cortex in adult humans induced by flickering at 8 Hz. Using a novel multi-speckle detection system which allows to resolve small functional changes of the decay time of the DWS autocorrelation function, we find enhanced dynamics in the visual cortex upon stimulation in a group of 9 subjects.

2. Methods

DWS experiments were performed in transmission geometry with two fiber-optic probes with source-receiver distances of 16 mm (short-distance probe) and 30 mm (long-distance probe) which were placed on the head of the subject over the occipital lobe (between positions O1 and O2 in the international 10-20 system for EEG [21]; see Fig. 1). Light from a diode laser operating at a wavelength of 802 nm (Toptica TA 100) was coupled into a multi-mode fiber whose output was expanded to reach $4\,\mathrm{mW/mm^2}$ on the scalp surface. Multiply scattered light was collected with bundles of $N = 23$ and $N = 2$ few-mode fibers [22] (for the long and the short source-receiver distances, respectively). The output of each fiber was coupled to an avalanche photodiode (Perkin-Elmer SPCM-AQ4C) whose TTL pulse output was used to compute the intensity autocorrelation function by a custom-built 32-channel autocorrelator (correlator.com) with an integration time of 26 ms. The experimental setup is schematically shown in Fig. 1. From the intensity autocorrelation function $g_i^{(2)}(\tau)$ measured by detector i the bundle-averaged

field autocorrelation function $g_{\mathrm{b}}^{(1)}(\tau) = \left[\frac{1}{N}\sum_{i=1}^{N}(g_i^{(2)}(\tau)-1)/\beta_i\right]^{1/2}$ was calculated, using experimentally determined coherence factors β_i (G. Dietsche et al., in preparation).

Nine female, healthy volunteers (age between 20 and 25 years, right-handed, without epilepsy history) recruited from students of the University of Konstanz took part in this experiment. The visual stimulation consisted in watching a CRT screen flickering at 8 Hz for 30 s. The distance between eyes and screen was approximately 80 cm (screen diagonal: 43.2 cm). During the baseline period of 30 s the subjects closed their eyes. Each baseline-stimulation block was repeated 5 times in a darkened room. During the experiment, the heartbeat rate was recorded with a pulse oxymeter (Nellcor N595). The study protocol was approved by the University's Ethical Review Board.

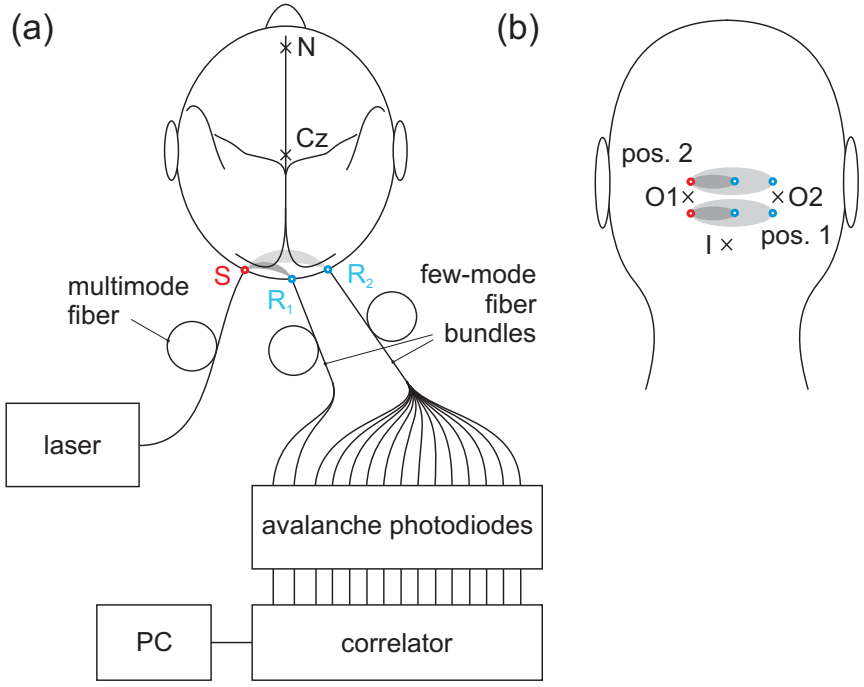

Fig. 1. (a) Schematic view of the experimental setup showing the positioning of the source fiber (S; red circle) and the receiver fiber bundles (R_1 and R_2 for short- and long-distance probes, respectively; blue circles). Light and dark grey shaded areas indicate the tissue regions sampled by the long- and by the short-distance probes, respectively. (b) Positioning of the DWS probes on the occipital cortex. I: inion, Cz: vertex, N: nasion.

Changes of the DWS autocorrelation function upon stimulation were quantified by the decay time of the bundle-averaged field autocorrelation function $g_{\mathrm{b}}^{(1)}(\tau)$,

$$\tau_{\mathrm{d}} = \int_{\tau_1}^{\tau_2} g_{\mathrm{b}}^{(1)}(\tau)\,\mathrm{d}\tau. \tag{1}$$

The lower integration limit is $\tau_1 = 4\times10^{-7}$s, and τ_2 is defined by $g_{\mathrm{b}}^{(1)}(\tau_2) = 0.1$. Our choice of the upper integration limit τ_2 aims at suppressing contributions from short photon paths which do not carry information on the cortex, and, secondly, at reducing the noise in the decay time [23].

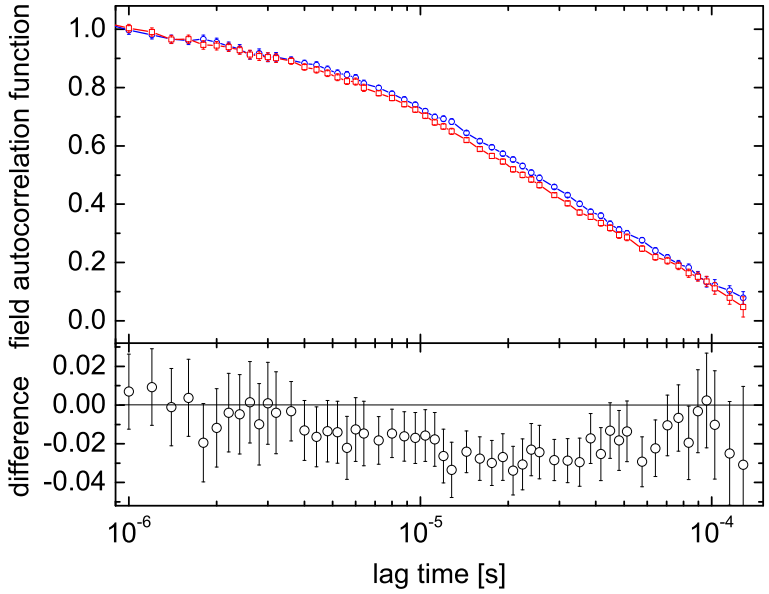

Fig. 2. Top: bundle-averaged field autocorrelation function $g_{\mathrm{b}}^{(1)}(\tau)$, measured over the primary visual cortex, from one subject for baseline (blue circles) and visual stimulation periods (red squares). Bottom: difference $\Delta g_{\mathrm{b}}^{(1)}(\tau) = g_{\mathrm{b,stimulation}}^{(1)}(\tau) - g_{\mathrm{b,baseline}}^{(1)}(\tau)$ as a function of lag time τ. The probe with 30 mm source-receiver spacing was located above the inion at 10% of the inion-nasion distance. The error bars represent the standard deviation over 5 blocks. For clarity, only data for lag times $\tau < 1.3 \times 10^{-4}$s are shown. The average relative decay time $\tau_{\mathrm{s/b}}$ is 0.955. Total integration time: 150 s. Count rate per fiber mode: 3.5 kHz.

3. Results

Figure 2 shows the bundle-averaged field autocorrelation function $g_{\mathrm{b}}^{(1)}(\tau)$ from one subject, as a function of the lag time τ, measured with the long-distance receiver for baseline and stimulation periods. During the stimulation period, the decay of the autocorrelation function is faster, indicating that the dynamics in the visual cortex area probed by the DWS experiment is accelerated, such as by an increase in CBF. The difference of field autocorrelation functions $\Delta g_{\mathrm{b}}^{(1)}(\tau)$ can be resolved for a range of lag times $4\,\mu\mathrm{s} \leq \tau \leq 50\,\mu\mathrm{s}$, with a pronounced minimum $\Delta g_{\mathrm{b}}^{(1)} = 0.033 \pm 0.013$ at $\tau = 20\,\mu$s. The relative decay time defined by $\tau_{\mathrm{s/b}} = \tau_{\mathrm{d,stimulation}} / \tau_{\mathrm{d,baseline}}$ is 0.955.

The measurements were carried out successively on two positions above the inion: position 1 located at 10% of the inion-nasion distance and position 2 at 15% of this distance (see Fig. 1b). In the group average, the relative decay time $\tau_{\mathrm{s/b}}$ is smaller than unity (see Fig. 3). For the long-distance probe, we find $\tau_{\mathrm{s/b}} = 0.962$ and $\tau_{\mathrm{s/b}} = 0.970$ at position 1 and 2, respectively. For the short-distance probe, the ratios are $\tau_{\mathrm{s/b}} = 0.953$ and $\tau_{\mathrm{s/b}} = 0.950$ for position 1 and

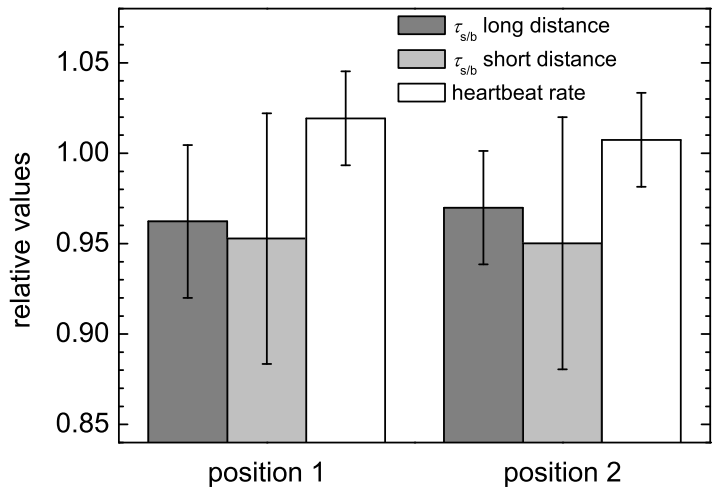

Fig. 3. Group average of the relative decay times $\tau_{s/b}$ measured with the long- and the short-distance probe, and of the heartbeat rate for positions 1 and 2 over the primary visual cortex. The difference of the heartbeat rate between positions 1 and 2 is due to the successive measurements at these two positions. The error bars represent the standard deviation of $\tau_{s/b}$ and heartbeat rate, respectively, over the 9 subjects.

2, respectively. However, a t-test shows that these changes in decay time are only marginally significant: $t(8) = -2.043$, $p = 0.075 > 0.05$ for position 1; $t(8) = -2.146$, $p = 0.064 > 0.05$ for position 2. This indicates that the source-receiver distance of 16 mm is not large enough for the DWS signal to contain contributions from cortical dynamics. The short-distance probe thus mostly samples scalp dynamics reflecting the peripheral perfusion.

On the other hand, for the measurements with the long-distance probe, a t-test shows that the stimulation leads to significant changes: $t(8) = -2.672$, $p = 0.028 < 0.05$ for position 1; $t(8) = -2.874$, $p = 0.021 < 0.05$ for position 2. This decrease in decay time for the data measured with the long-distance probe indicates that there is a significant enhancement in cortical dynamics when the visual cortex is activated by flickering. In Fig. 3, we also show the relative heartbeat rate during the stimulation periods. One can see a slight increase in the heartbeat rate: 1.9% for position 1 and 0.7% for position 2. Nevertheless, these changes are not significant: $t(8) = 0.9907$, $p = 0.351 \gg 0.05$ for position 1; $t(8) = 0.8525$, $p = 0.419 \gg 0.05$ for position 2.

4. Discussion

PET measurements on the primary visual cortex show that 8 Hz flickering induces an increase both in CBF and CBV by about 68%, and 21%, respectively [19]. The increased CBF results in enhanced cortical dynamics which contributes to the faster decay of the autocorrelation function, as observed in our experiments. On the other hand, an increase in CBV must be reflected by a reduction of the transmitted light intensity. Indeed, this was observed in our experiments: during flickering periods, the average photon count rate recorded with the long-distance receiver

decreases by about 2.49% for position 1, and by 2.26% for position 2.

These changes are roughly in line with model calculations with a three-layer head model (modelling the cortex as semi-infinite) [12]: an increase of the cortical absorption coefficient by 21% is predicted to lead to a 2.88% decrease of transmitted light intensity recorded with a source-receiver distance of 30 mm.

Modelling the dynamics in scalp and cortex by Brownian motion, an increase in the cortical diffusion coefficient by 68%, together with a 21% increase in cortical absorption, results in a decrease of the decay time by about 2.37%, slightly smaller than the experimental decrease (3.77% for position 1, and 3.01% for position 2). In our model calculation, optical parameters for each layer were taken from the literature [24], and values 0.56 cm and 0.63 cm for the thickness of scalp and skull, respectively, were assumed. Baseline effective diffusion coefficients for scalp and cortex were assumed to be $5.0 \times 10^{-9}\,\mathrm{cm}^2/\mathrm{s}$. The differences between the decay time calculated with the 3-layer model and the measured ones might be due to inaccurate values of the thicknesses of scalp and scull, or due to the modelling of erythrocyte motion by diffusion. It should be noted that that a CBV increase has two effects with opposite directions on the DWS decay time: an increase in CBV gives rise to increased cortical absorption, which changes the path-length distribution in tissue by cutting off the long paths. This causes the decay time to increase. On the other hand, as more erythrocytes enter the sampled volume, the number of scattering events contributing to the autocorrelation function increases by the same percentage as the CBV. This increase in the 'effective scattering events' results in a faster decay of the autocorrelation function.

The correlation coefficient r between the relative decay time of the autocorrelation function and the relative photon count rate were also computed for the long-distance probe data across the 9 subjects: $r = 0.688$ for position 1, and $r = 0.585$ for position 2. This positive correlation between changes in CBF and CBV is consistent with the hemodynamical response pattern observed in the activated visual cortex with PET [19].

During stimulation periods, we observed a slight increase in the average heartbeat rate. Nevertheless, this does not account for the functional reduction of the DWS decay time observed with the long-distance probe, as (i) the heartbeat change is not significant ($t(8) = 0.991$, $p = 0.351$ for position 1; $t(8) = 0.853$, $p = 0.419$ for position 2); (ii) not all subjects showed an increased heartbeat rate during stimulation: in 3 of 9 subjects the heartbeat rate was found to slightly decrease during stimulation periods, yet the faster decay was still observed; (iii) the correlation between the relative heartbeat rate and the relative decay time $\tau_{s/b}$ is not significant ($t(7) = -2.104$, $p = 0.074$ for position 1; $t(7) = -1.018$, $p = 0.455$ for position 2). The absence of heartbeat rate changes upon stimulation is consistent with the DWS decay times of the superficial layers measured with the short-distance probe. This is in contrast to motor stimulation by finger opposition where the peripheral perfusion and the heartbeat rate are accelerated along with the cortical dynamics [12, 15]. The observation that the dynamics within the visual cortex is enhanced during the flickering periods even though the heartbeat rate remains constant indicates that the acceleration of the DWS signal from the visual cortex is mainly determined by the functionally increased blood flow velocity and not by shear deformations within cortical tissue induced by pulsatile volume variations of the vessels.

5. Conclusions

Fiber-based multi-speckle detection allows to detect the functional activation in the human visual cortex elicited by 8 Hz flickering in an entirely non-invasive way in individual subjects. Flickering leads to a reduction of the decay time of the DWS autocorrelation function of about 4% in a group of 9 subjects. This effect is by about 42 % larger than the change of transmitted intensity reflecting the functional change of blood volume. Our data indicate that the functional

DWS signal is determined by the regional blood flow velocity and not by shear deformations within cortical tissue.

In conjunction with near-infrared spectroscopy, the high sensitivity and temporal resolution of DWS to cortical perfusion could be used for mapping metabolism in the human brain non-invasively in real time. This might be useful for situations not allowing the use of conventional methods such as MRI or PET, such as in neuro-intensive care or in neuro-rehabilitation.

Acknowledgments

We thank E. Keller, M. Wolf, B. Rockstroh and J. Kissler for helpful discussions, and G. Maret for continuous support. This work is funded by the Deutsche Forschungsgemeinschaft (DFG), the Landesstiftung Baden-Württemberg, and the Center for Applied Photonics (CAP) Konstanz.